JOURNAL OF THE KOREAN ASTRONOMICAL SOCIETY
26: 33 ~ 45, 1993

SURFACE PHOTOMETRY OF NGC4419

CHOI, JEONG TAE, ANN, HONG BAE, AND LEE, HYUNG MOK
Department of Earth Sciences, Pusan National University, Pusan 609-735
(Received March 25, 1993; Accepted April 20, 1993)

ABSTRACT

We have conducted surface photometry of a spiral galaxy NGC4419, by making use of photographic plates in U, B, V and R-bands taken by 105 cm Schmidt Camera at Kiso Observatory. Two dimensional surface brightness distributions as well as luminosity profiles along the major axis are examined in detail to decipher the morphological properties of the galaxy. Analysis of the color distributions of NGC4419 shows that $B-V$ and $U-B$ colors remain constant throughout the galaxy with a weak trend of blue bulge in $B-V$ color. The blue bulge might indicate an active star formation in the nucleus of NGC4419. For a quantitative analysis of the luminosity distribution of NGC4419, the observed luminosity profiles are decomposed into bulge and disk components, assuming the bulge component to follow de Vaucouleurs $r^{1/4}$-law while the disk component is assumed to be exponential. The fitting generally fails at the central part and at the shoulder near $r = 15''$ where bulge and disk components overlap. The failure at the central part cannot be attributed wholly by the seeing disk since the core-radius of the central plateau is much larger than the width of point spread function. The failure at shoulder could be due to the luminosities from the spiral arms.

Key Words: galaxies, photometry, barred, structure.

I. INTRODUCTION

The photographic plates are being replaced by CCD chips because of high sensitivity and superior linearity of CCD. However, large format CCD chips are still very rare so that the surface photometry of large galaxies often require photographic observations. Furthermore, it is usually possible to search existing plates to do photometric study of most objects since most of the sky accessible to wide angle telescopes are already surveyed.

We have been studying the physical characteristics of barred spiral galaxies mostly using Kiso plate library (e.g., Ann 1986; Ann and Lee 1987). In an attempt to widen our data base for the surface brightness distribution of such type of galaxies, we have chosen NGC4419 which is classified as SBa in Second Reference Catalogue of Bright Galaxies (abbreviated as RC2 hereafter; de Vaucouleurs, de Vaucouleurs and Corwin 1976). NGC4419 is located in the Virgo cluster and the distance of this galaxy is assumed to be about 20 Mpc (Kent 1988).

This galaxy has been studied by several investigators: For example, Rubin et. al (1985) determined the rotation curve and Kent (1988) made a CCD photometry from which he studied the average luminosity profile. However, detailed brightness distribution at several wavelengths has not been carefully studied yet.

In the present study, we will analyze the luminosity distribution of NGC4419 in four wavelengths (U, B, V and R-bands), based on the surface photometry from the 6 Kiso plates. In order to understand the physical characteristics of the galaxy, iterative profile decomposition technique will be applied, by assuming de Vaucouleurs' $r^{1/4}$-law for bulge component and exponential function for disk.

Most of the data reduction in the present study was done with IRAF (Image Reduction and Analysis Facility) package developed at the NOAO (National Optical Astronomical Observatories) and SPIRAL (Surface Photometry Interactive Reduction and Analysis Library) software developed at Kiso Observatory. These two packages were combined together so that they can be run under IRAF user interface. A brief introduction to SPIRAL/IRAF will be found elsewhere (Ann 1993).

Table 1. The Plates Used in the Present Study and Observational Log

Plate No.	Band	Observer	Date	Exp. (min.)	Emulsion	Filter
L02078	U	Kodaira et al.	2/28/1979	90	IIa-O	UG
L06108	B	Mizuno	2/6/1989	70	IIa-O	GG385
L03736	B	Noguchi and Kondo	5/17/1982	30	IIa-O	GG385
L05732	V	Mizuno Hamabe	2/28/1988	60	IIa-D	GG495
L03685	V	Hamabe et al.	3/22/1988	30	IIa-D	GG495
L02079	R	Kodaira et al.	2/28/1979	60	103a-F	RG610

This paper is organized as follows: In the immediately following section, we describe the basic procedure to obtain luminosity distributions from photographic plates. The derived luminosity distributions in multi-wavelengths are presented and analyzed in §III. The procedure of profile decomposition and its results are presented in §IV. The final section summarizes our major findings of the present work.

II. THE PLATE MEASUREMENTS AND DATA REDUCTION

The plates used in the present study were taken at Kiso Observatory using 105 cm Schmidt telescope. We have used two plates taken with different exposure times for B and V bands in order to increase the dynamic range of the surface brightness distribution. Therefore total number of plates used in the present study was 6. The observational log and the short description of the plates are given in Table 1.

(a) Plate Density and Intensity Scale

The blue luminosity diameter of NGC 4419 is 203.3 seconds of arc (RC2), which is translated to be about 3.25 mm in plates. However, we have scanned 1.6cm x 1.6cm area centered on the nucleus of NGC 4419 in order to cover sufficient area. This will enable us to determine the sky brightness accurately.

The plates were scanned by the PDS 2020 GMS microdensitometer at Kiso Observatory with aperture size of 17μm. The sampling interval between two successive points was 16 μm. In the scanning we have used the 'raster mode' in which the x-directional scan was made both from left to right (positive scan) and from right to left (negative scan). This technique ensures the accurate sampling of surface brightness data. The scanning speed was 150 in PDS units. The total scan time was about 30 minutes for each plate.

In order to translate the density of the plate to intensity scale, we have also scanned four wedges located at four boundaries of each plate. The wedges were exposed to known 15 different intensities after the plates taken, with the same exposure time. The scan area of each wedge was 1 cm x 12 cm, and the sampling intervals were 50 μm and 500 μm for x- and y-directions, respectively.

From the wedge data, we have determined the relation between the photographic density and the intensity of the light. This relation is known as a 'characteristic curve'. The characteristic curve was fitted to 'Goad function' which has the form

$$\log I = P_0 + P_1 \times Y + P_2 \times Y^2 + P_3 \times Y^3,$$

where

$$Y = D + P_4 \times \log\left(1 - 10^{-D}\right).$$

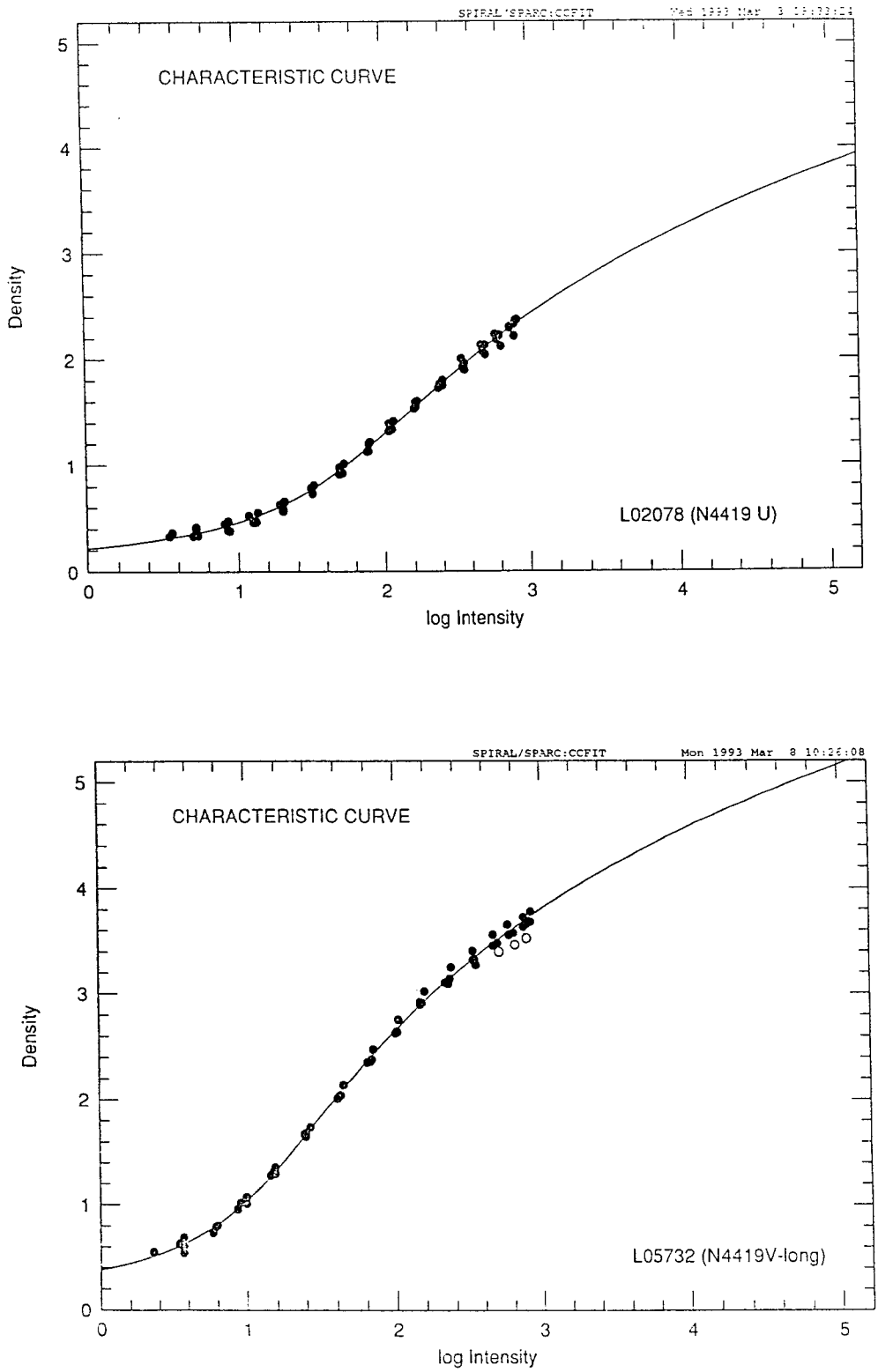

Fig. 1. Characteristic curves for the U and V plates. The filled circles are the data and the solid line is best fit Goad function. The open circles in V plate are those rejected from the Goad function fitting because of their large deviations from the mean relationship.

Here, I is the intensity of the light (which is wedge constant) and D is the measured plate density. P_0 through P_4 are adjustable constants to be determined by fitting the data to the Goad function via least-squares method. We present the characteristic curves of the U- and long-exposure V-band plates in Figure 1 where the solid line represents the Goad function fitting. Characteristic curves of the other plates are not presented because they are nearly the same as that of the V-plate in Figure 1. The open circles are the data from one wedge which was rejected in the fitting because of large deviation from other data set.

We may define three quantities for the characteristic curves. The 'contrast' basically measures the slope of the curve in the linear regime. The small change in intensity can easily be recognized in high contrast plates. The 'dynamic range' is the ratio between high and low ends of the linear regime in the characteristic curve. If the slope of the characteristic curve is nearly constant, the plate is said to have good 'linearity'. Generally speaking, the V-band plate shows rather good linearity and large dynamic range. This is one of the reasons why Kodaira et al. (1990) adopted V as the band for the northern sky survey. Although there seems to be a weak sign of saturation in the long-exposure V-band plate, it does not introduce a significant error to the derived intensity as long as there is no inhomogeneity in the plate and no severe over-exposure.

(b) Sky Brightness and Relative Intensity

The photographic density distribution $D(x, y)$ now can be translated to intensity distribution $I(x, y)$, which is the sum of galaxy brightness ($I_G(x, y)$) and the sky brightness ($I_S(x, y)$). Therefore we have to subtract $I_S(x, y)$ from $I(x, y)$ in order to determine $I_G(x, y)$.

The surface brightness distribution of the sky may be determined by averaging the brightness of several places where there is no star or galaxy. However, the sky brightness distribution could have systematic gradient over large area of sky due to the large scale distribution of stars and background galaxies. In order to account such a possibility, we have fitted the sky brightness distribution to a two-dimensional first order polynomial

$$I_S(x, y) = ax + by + c.$$

The coefficients a, b and c have been determined by least-squares fitting to the sky brightness data taken at several points over the scanned area.

The relative intensity is the brightness of the galaxy relative to the sky brightness. Therefore

$$I_{rel}(x, y) = [I(x, y) - I_S(x, y)] / I_S(x, y).$$

The relative intensity distribution could show large fluctuation at the outer parts of the galaxy mainly due to the peculiarity of the photographic emulsion or errors introduced during the development of the plate. In order to reduce such noise, smoothing technique is used. There are several algorithms for smoothing in SPIRAL/IRAF package. We have used the 'variable Gaussian smoothing', in which the width of the smoothing kernel of Gaussian function varies according to the signal-to-noise ratio. This method retains the original image for the area of high signal-to-noise ratio while significant smoothing is done in the noisy areas.

The relative brightness distribution contains the contributions from the stars and other galaxies. We also have performed cleaning which basically removes the unwanted contribution of stars and galaxies. The cleaning is done by fitting the brightness distribution of area that contains a galaxy or a star to smooth polynomial and removing the small wavelength components (i.e., a star or a galaxy).

III. LUMINOSITY DISTRIBUTION

The global morphological properties of NGC4419 were examined by the isophotal maps, as shown in Figure 2, and the density maps on SAOimage. The ratio between minor and major axes of disk varies from plate to plate, but the average value is about 2.7 which corresponds to ellipticity of 0.63 (Figure 5). If we assume that the galaxy has circular disk, the inclination angle is about 68°. Such a high inclination angle makes it difficult to analyze the two-dimensional structure such as spiral arm and bar. NGC4419 has been known to have a bar (de Vaucouleurs, de Vaucouleurs and Corwin 1976),

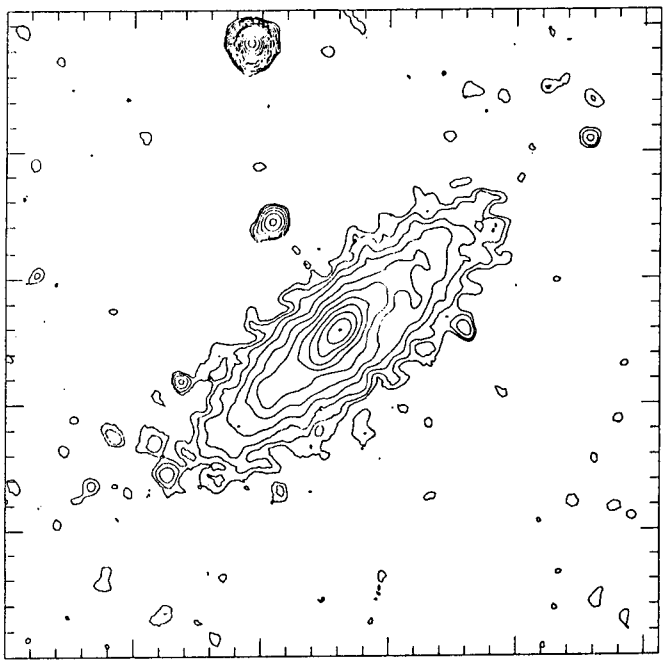

NGC4419 U

(a)

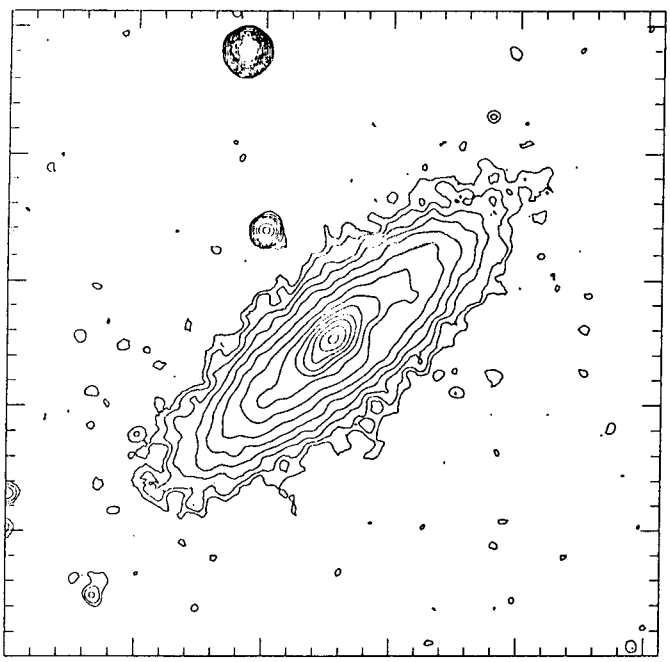

NGC4419 B-long

(b)

Fig. 2. Isophotal maps of NGC4419 at (a) U, (b) B (long exposure) bands. The intervals of isophotes are 0.5 mag and the outermost isophote is 3 mag below the surface brightness of the sky. North is at top and east at left.

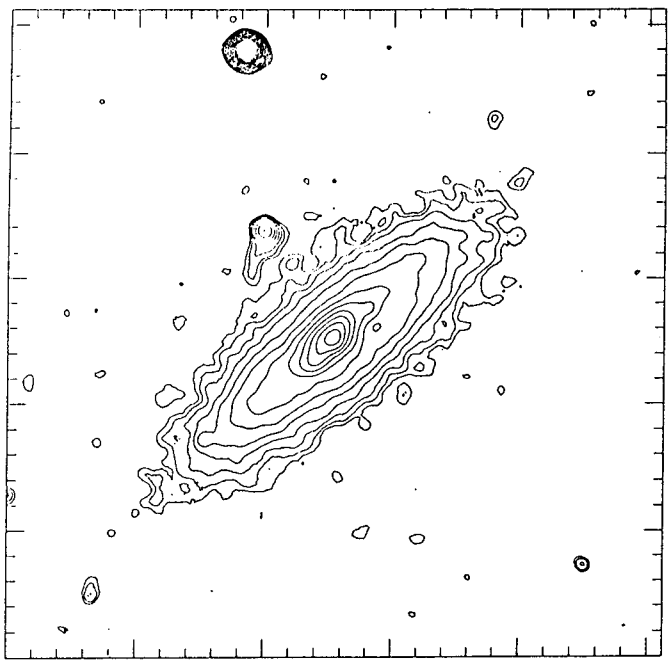

NGC4419 B-short

(c)

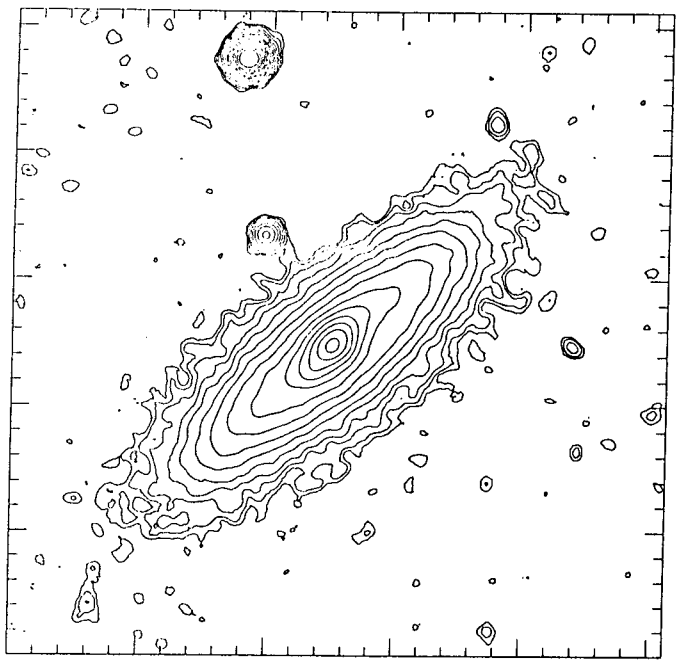

NGC4419 V-long

(d)

Fig. 2. Continued: at (c) B (short exposure), (d) V (long exposure) bands

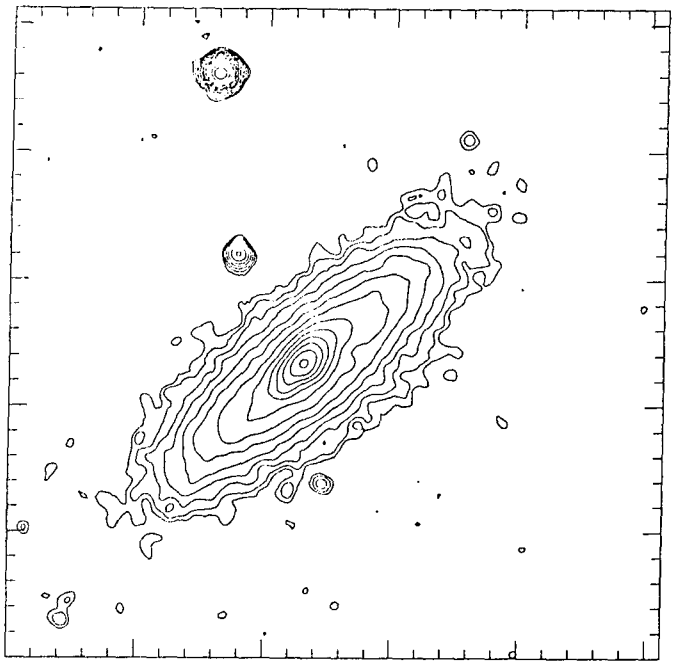

(e)

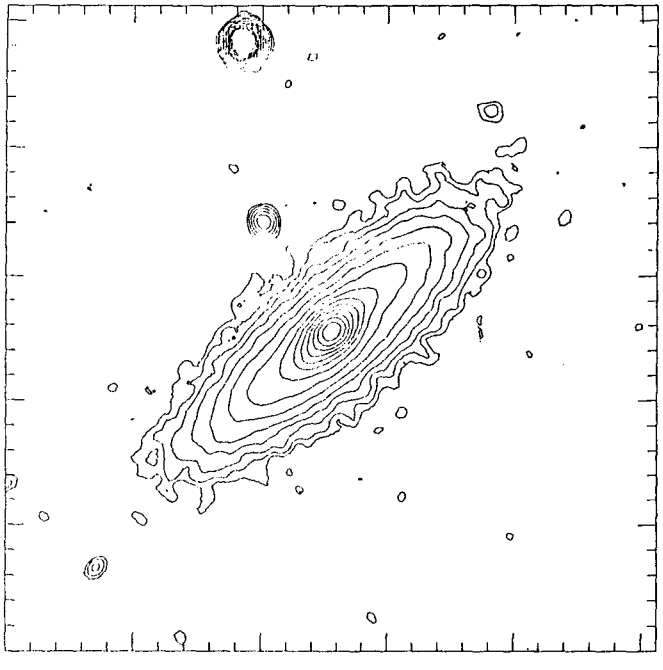

(f)

Fig. 2. Continued: at (e) V (short exposure) and (f) R bands.

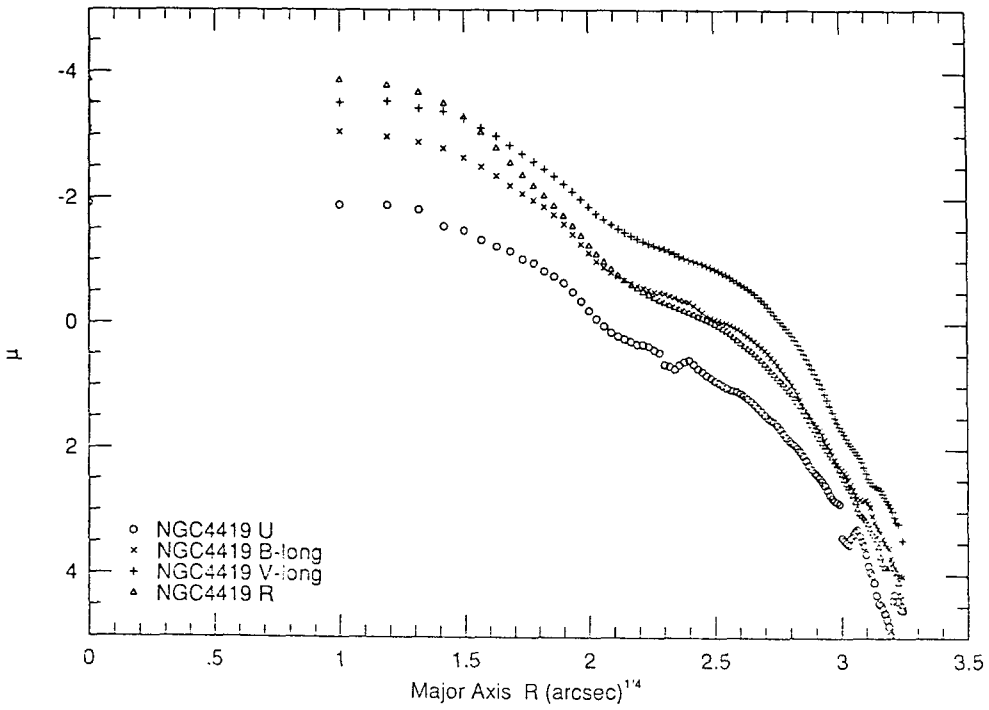

Fig. 3. Distribution of surface brightness in units of sky brightness as a function of the major axis after ellipse fitting at U, B (long exposure), V (long exposure) and R bands.

but a detailed examination of the isophotal maps and density maps with high contrasts showed that the central elongated feature is a spiral arm which emerges from near the nucleus of the galaxy. Recent morphological investigation using CCD images also showed that it should be classified as a normal spiral galaxy (van den Bergh, Pierce and Tully 1990).

More quantitative morphological study can be done by using one-dimensional brightness profile. We have used ellipse fitting method in SPIRAL which was developed by Kent (1983) to determine the luminosity profiles along the major axis together with the ellipticity and position angle (abbreviated as PA hereafter) of the isophotes. In the ellipse fitting technique, the observed isophotes are fitted to sets of concentric ellipses. PA is defined as the angle measured counter-clockwise from the north and ellipticity is $1 - a/b$ where a and b are the semi-major and semi-minor axes, respectively.

The major axis profiles obtained by the ellipse fitting technique are presented in Figure 3. In these figures, we have used the surface brightness scale (i.e., $\mu = -2.5\log I_{rel}$) instead of the relative intensity. Therefore, $\mu = 0$ corresponds to the surface brightness of the galaxy equivalent to the sky brightness. It is evident in these figures that the profiles are composed of more than two distinct components: the central part showing steep rise toward the nucleus and the smoother outer part with a change of slope near $r = 60''$. The profile in R-band shows steeper variation of the surface brightness in the central part than any other profiles. The profiles become rather erratic near $\mu > 5$ where the surface brightness of the galaxy is less than 1% of the sky brightness.

The behavior of PA against the major axis is plotted in Figure 4. PA varies smoothly throughout the galaxy but settles to about 130° for $r > 40''$ where disk component dominates. For $r < 5''$, PA varies abruptly. The main reason for the rapid change in PA is believed to be related to the ellipticity. For the ellipses with small ellipticity, the position angle is poorly determined. Since the ellipticities of the inner contours are small, the PA becomes rather erratic. The variation of PA between $r = 10''$ and $r = 20''$ is caused by the inner spiral arm which is most pronounced in U-band.

Figure 5 shows the variation of ellipticity along the major axis of NGC4419. It decreases rapidly from the nucleus to $r = 10''$ where the inner spiral arm seems to emerge. The nearly constant ellipticity between $r = 10''$ and $r = 20''$ for U- and B-band images is due to the inner spiral arm. The variation of ellipticity and PA between $r = 20''$ and $r = 35''$

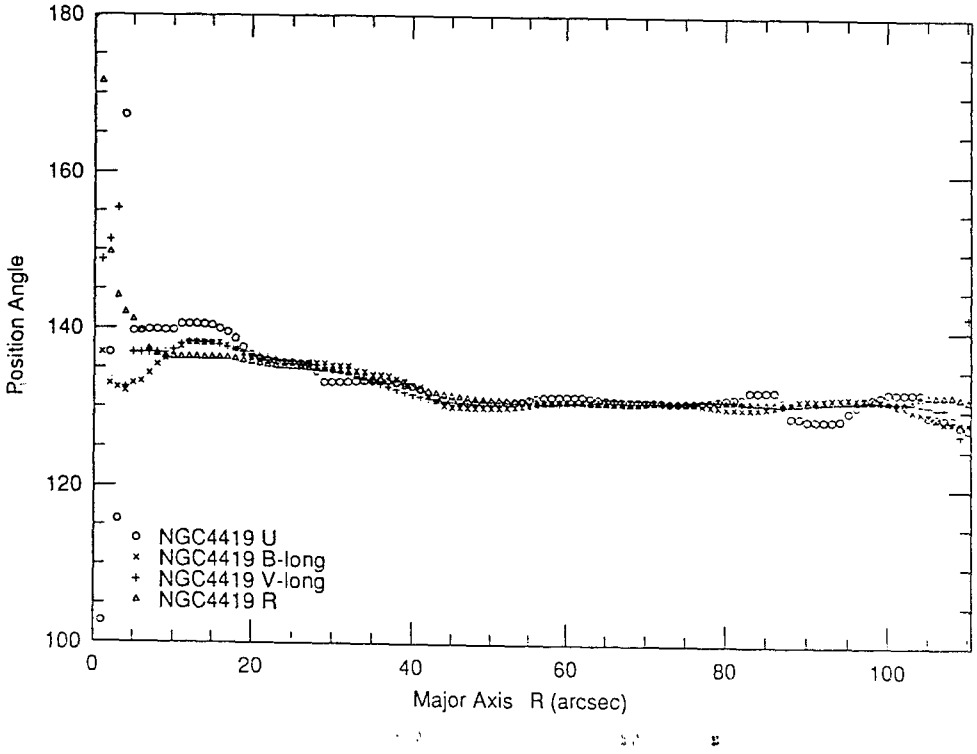

Fig. 4. Distribution of the position angles of major axis as a function of the major axis R.

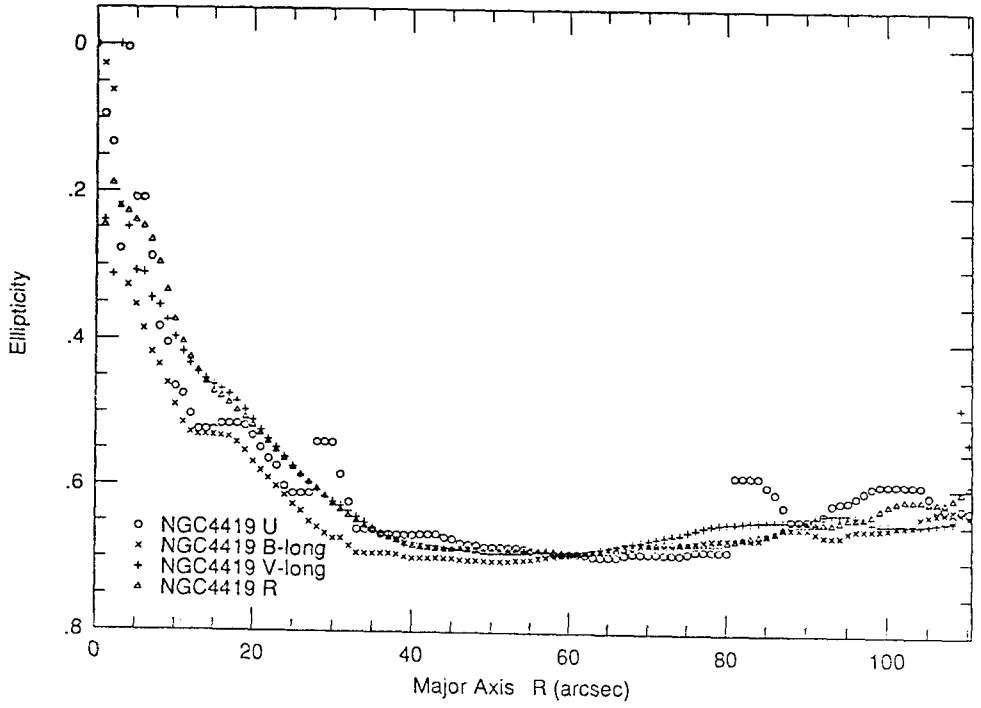

Fig. 5. Distribution of ellipticities of the contour levels as a function of the major axis. Note that the ellipticity generally becomes smaller at small radii indicating the dominance of bulges.

indicates that there are components other than bulge and disk. Bar and/or lens are plausible candidates for the extra components but it is not clear which is the real cause of the extra luminosity.

The color distributions can also be inferred from Figure 3. There seems to be no significant variation in $B-V$ and $U-B$ colors over a large range of radii except the slightly bluer $B-V$ color for $r < 20''$. However, colors including R magnitude, say $V-R$ color becomes redder and redder toward the nucleus of the galaxy. This is due to the steep rise in the luminosity of R-band toward the nucleus as shown in Figure 3. The reason for this steep rise in the R-band profile is unclear. However, it may be caused by, at least in part, the emission lines such as H_α, NII, and SII because the the nucleus of NGC4419 is known as LINER (Low Ionization Nuclear Emission Regions) and it has a small gaseous disk around the nucleus (Kenney et al. 1990). We expect active star formation in this disk which accompany strong emission lines.

IV. PROFILE DECOMPOSITION

We have determined one-dimensional brightness profiles from two-dimensional luminosity distribution of the galaxy. We now attempt to decompose the luminosity profiles into two components: a bulge and a disk. Most of the spiral galaxies are known to have distinctive bulge and disk components. The surface brightness of the bulge component generally follows de Vaucouleurs' $r^{1/4}$-law, i.e.,

$$\mu_{bulge} = \mu_e + 8.325\left[(r/r_e)^{1/4} - 1\right]$$

where r_e is the 'effective radius' and μ_e is the effective surface brightness. The disk component can usually be represented by the exponential disk of Freeman (1970). In terms of surface brightness,

$$\mu_{disk} = \mu_0 + 1.082(r/h),$$

where μ_0 is the central surface brightness of the disk and h is the scale length.

The observed profiles can be decomposed into these components by least-squares method. There are four adjustable parameters: μ_e, r_e, μ_0 and h. Because the parameters in fitting functions are generally non-linear, we have used the iterative method (Kormendy 1977) in determining these parameters. The precise procedures are described below.

We first use the data in the outer parts to determine μ_0 and h by assuming that the profile is exponential (i.e., disk only). We then subtract the extrapolated disk component from the observed profile to determine the bulge component. The bulge component obtained this way is fitted to de Vaucouleurs' formula. Then we subtract this bulge component from the observed profile to obtain net disk component. This circular procedure is repeated until the adjustable parameters vary very little. This technique gives convergence in 4-5 iterations when the required relative error is less than 1%.

We tried to decompose the major axis profiles into bulge and disk components, but it was not successful except for the R-band profile which differs from the other profiles in the central part. The reason for the failure of decomposition is quite evident from Figure 3 where we plot the surface brightness of major axis as a function of $r^{1/4}$. Except for the R-band profile, the radii where the profiles seem to follow the de Vaucouleurs' law are very limited and the slopes of the profiles are too shallow to be adequately decomposed. Moreover, unresolved components which are mentioned in §III make the profiles more difficult to be properly decomposed.

But, it was possible to decompose the mean surface brightnes into bulge and disk components as shown in Figure 6. Because mean surface brightness profile is an azimuthally averaged luminosity distribution along the radius, the effect of secondary components such as spiral arm on the profile decomposition is negligible. The mean radius in Figure 6 is defined as $r \equiv (ab)^{1/2}$ where a and b are semi-major and semi-minor axis, respectively. The best fitting parameters are also shown in the figures. As can be seen in these figures the two-component fitting gives quite a good result except for the very central part of the galaxy and the transition region near $r = 15''$.

The central parts of the luminosity profiles are vulnerable to the overexposure and heavily affected by the instrumental and atmospheric point spread function. However, the discrepancies in the central part can not be soly explained by the combined effects of seeing convolution and overexposure. For the sizes of seeing disks from stellar images are 2-3 seconds of arc which are smaller than the observed core radius of about 5 seconds of arc. Moreover, there is little sign of overexposure in B and R-band images, even for the core of the galaxy.

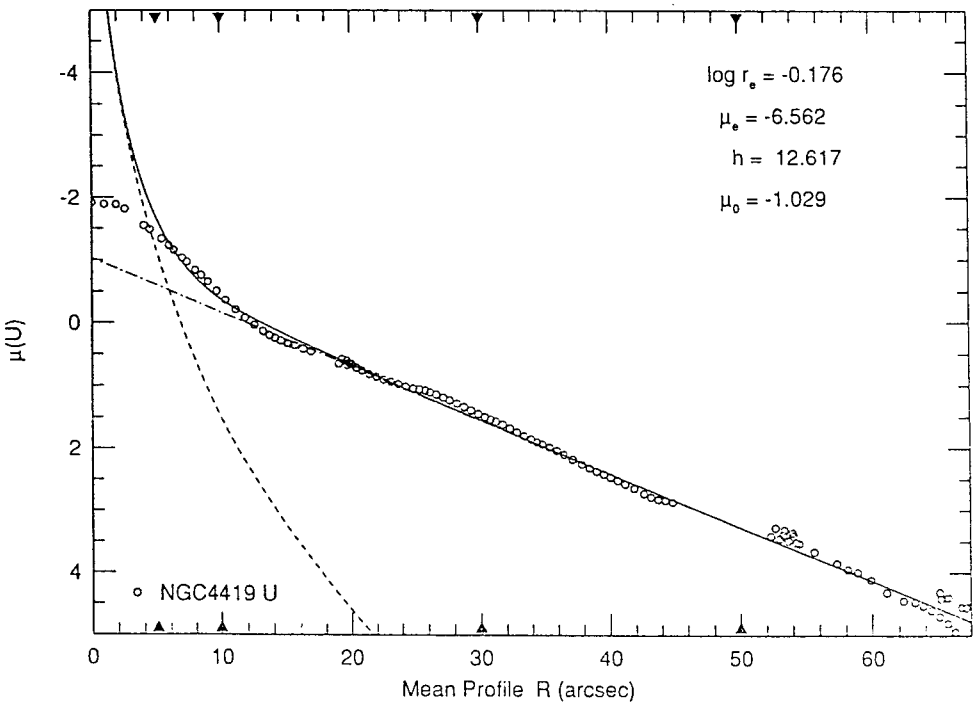

(a)

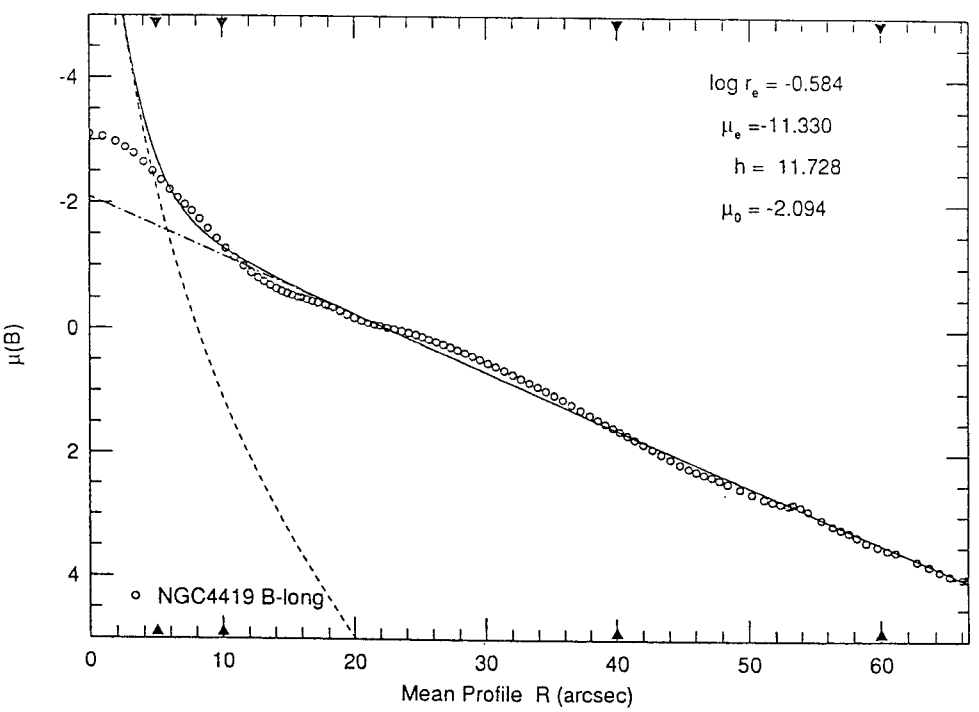

(b)

Fig. 6. Profile decomposision of mean profiles at (a) U, (b) B (long exposure) bands. The decomposition parameters are shown in the figures.

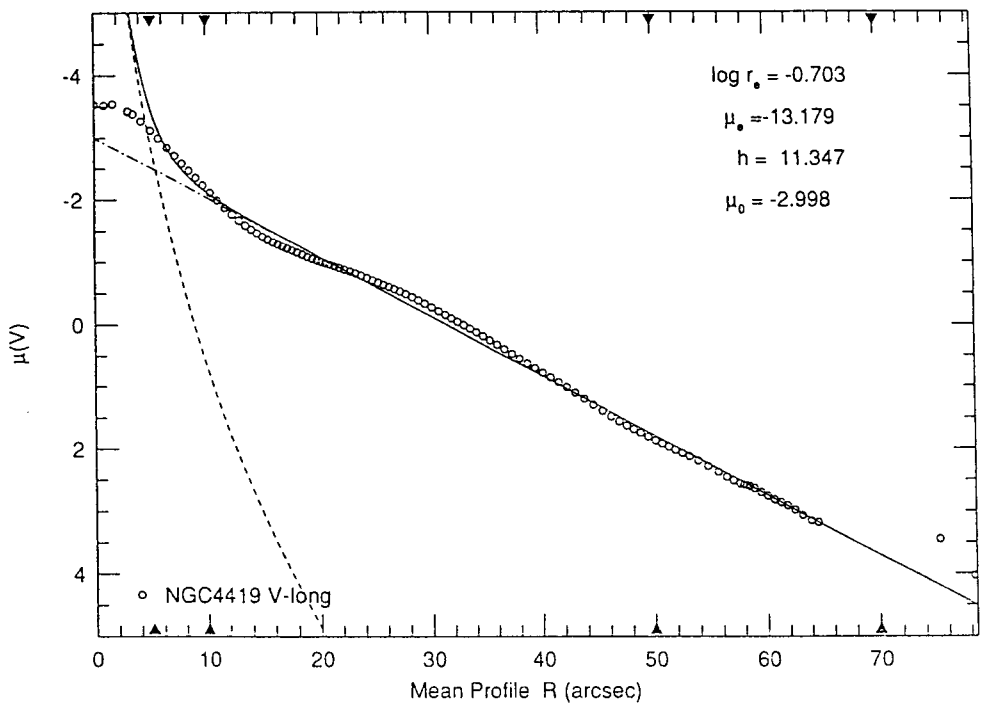

(c)

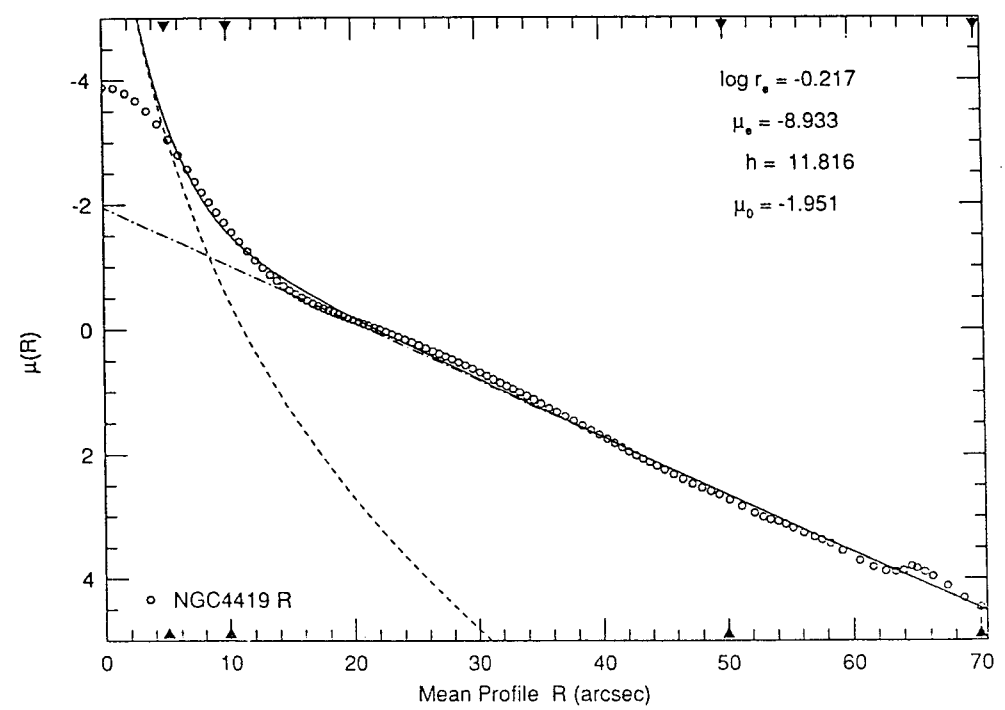

(d)

Fig. 6. Continued: at (c) V (long exposure) and (d) R bands.

V. SUMMARY AND CONCLUSION

Surface photometry of a spiral galaxy NGC 4419 is made using the plates taken at Kiso Observatory. The plates are scanned by PDS microdensitometer. The photographic densities are converted to intensity using the wedge data. The surface brightness image data are cleaned for foreground stars and background galaxies and smoothed the cleaned images to increase the signal-to-noise ratio.

Morphological properties of NGC4419 is examined in detail by using the isophotal maps and luminosity profiles in U, B, V, R wavebands. NGC4419 has been known as a barred spiral galaxy but our analysis shows that there is no bar but a spiral arm emerges near the nucleus. The R-band profile shows steeper rise of the surface brightness toward nucleus than other profiles. The reason for this steep gradient in the R-band surface brightness profile is not known, but, there is a possibility that the excess luminosity in R-band might be caused by, at least in some part, the emission lines in this waveband, such as H_α, NII, and SII.

There is no significant variation of $B-V$ and $U-B$ colors over the entire galaxy, but there is a mild trend of blue bulge, especially in $B-V$ color. If this blue color in the central part of the galaxy is real, it suggests an active star formation in the nucleus and surrounding gaseous disk observed by Kenney et al. (1990). This is also consistent with the nature of NGC4419 as a LINER. Therefore, it is highly desirable to map the H_α emission lines from the central part of the galaxy to confirm the star forming activity in and around the nucleus of NGC4419.

The mean surface brightness profiles are decomposed into a bulge that follows de Vaucouleurs' profile and a disk that follows Freeman's exponential disk. The fittings well reproduce the observed profile except for the the central part of the galaxy.

ACKNOWLEDGEMENTS

This research was supported in part by the Korea Research Foundation. We thank to KAO for the partial support of the travel to the Kiso Observatory. We are grateful to the staff of Kiso Astronomical Observatory for providing plate materials for the present study. H.B. Ann thanks to the hospitalities of DAO where part of the manuscript was wirtten duing his stay as a visiting astronomer.

REFERENCES

Ann, H. B., 1986, J. Kor. Astron. Soc., 19, 69
Ann, H. B., 1993, in preparation
Ann, H. B., & Lee, S.-W., 1987, J. Kor. Astron. Soc., 20, 49
Freeman, K. C., 1970, ApJ, 160, 811
Kenney, J. D. P., Young, J. S., Hasegawa,T., & Nakai, N., 1990, ApJ, 353, 460
Kent, S. M., 1983, ApJ, 266, 562
———— ., 1988, AJ, 96, 514
King, I. R., 1966, AJ, 71, 64
Kodaira, K., Okamura, S., & Ichikawa, S., 1990, Photometric Atlas of Northern Bright Galaxies (Univ. of Tokyo Press: Tokyo)
Kormendy, J., 1977, ApJ, 214, 359
Longo, G., & de Vaucouleurs, G. A., 1983, A General Catalogue of Photometric Magnitude and Colors in UBV Systems (U. of Texas Press: Austin, Texas)
Okamura, S., 1988, PASP, 100, 524
Rubin, V. C, Burstein, D., Ford, W. K., Jr., & Thonnard, N., 1985, ApJ, 233, 23
van den Bergh, S., Pierce, M. J., & Tully, R. B., 1990, ApJ, 359, 4